

Fabrication and analysis of plastic hypodermic needles

H. KIM and J. S. COLTON*

G.W. Woodruff School of Mechanical Engineering and Center for Polymer Processing, Georgia Institute of Technology, Atlanta, GA 30332-0405, USA

(Received 13 May 2004; in final form 17 June 2004)

Plastic hypodermic needles may help reduce illness and disease due to unsterile re-use, as they may be more easily disabled and disposed of as compared to metal ones. This paper presents the fabrication of plastic hypodermic needles using micro-injection moulding and the analyses of their buckling behaviour. As a needle cannula is a thin-walled column (here 0.7 mm outer diameter with a 0.15 mm wall thickness), it is vulnerable to buckling. The buckling behaviour is characterized by numerical simulation and experiments, which are compared to the penetration forces for rubber skin mimic and human skin.

Introduction

In developing countries, an estimated 16 billion injections are given yearly. The World Health Organization (WHO) estimates that >21.7 million hepatitis B virus (HBV) (32% of new cases), >2 million hepatitis C virus (HCV) (40% of new cases), and >80 000 human immunodeficiency virus (HIV) (5% of new cases) infections occur *annually* due to unsafe injections [1, 2]. Most of this disease burden occurs in less developed countries where the appropriate sterilization and disposal of used needles and syringes are serious problems [3]. Conventional steel needle-plastic syringe combinations (needle-syringe) are a pressing problem for the developing world as (1) they are easily re-used without appropriate sterilization, (2) supply chains of new ones often are interrupted, and (3) proper medical waste disposal is lacking. The actual cost of the resulting disease burden has been estimated to be \$26 per injection in sub-Saharan Africa [4] and \$0.125 per injection globally [5], and to cause 9.2 million disability-adjusted life years (DALYs) between 2000 and 2030 [6]. In comparison, the acquisition cost of a needle-syringe is about 4¢.

To prevent their re-use, a number of auto-disable (A-D) needle-syringes have been developed. Typically these work by incorporating a ratchet-type mechanism or a metal clip which prevents the syringe's plunger from being withdrawn after injection has occurred, e.g., the Soloshot™, developed by Program for Appropriate Technology in Health (PATH) and marketed by BD [7]. The Uniject™, also developed by PATH and marketed by BD, is a single-use

injection system that consists of a metal needle attached to a pre-filled plastic blister (similar to a packet of mustard). WHO set a goal for A-D syringes to completely replace conventional needle-syringes in its immunization programs by the end of 2003 [8]. Other mechanisms, such as needle-shielding sheaths, have been developed to reduce the incidence of needle-sticks, another infection mechanism. While all of these devices, if used properly, reduce the chance of re-use and infection, most contain metal, which complicates the medical waste stream, as will be discussed below. Also, the elimination of unsterile re-use, ironically, will add to the number of needle-syringes requiring disposal.

The disposal of conventional needle-syringes is especially problematic, as very high temperatures (> 850°C) must be used to destroy or disable metal needles. In less developed nations, such incinerators are rare even in urban hospitals, let alone rural clinics. In the vast majority of the developing world, the used syringes are simply dumped behind the clinic or in landfills, easily accessible to children and animals.

Recycling is a means to 'dispose' of syringes safely and potentially profitably. The syringes, typically made from polypropylene, can be sterilized, shredded, and reprocessed into plastic products, such as car battery cases, automotive fenders, buckets, and lumber. Complicating factors for recycling are the metal needle, which sometimes is removed manually before the plastic can be recycled, resulting in needle sticks to the workers [9], as well as the metal in auto-disabling mechanisms.

*Corresponding author. Email: jonathan.colton@me.gatech.edu

A seemingly simple solution to these issues is a plastic hypodermic needle. A plastic needle can be dulled and sealed by the application of heat, such as from a candle flame, hot plate, or soldering iron. This would disable the needle, preventing its re-use and needle sticks. An all-plastic design eliminates metal thereby greatly simplifying the medical waste stream. Recycling would become a realistic option. The plastic first could be melted at approximately 200°C to render it sterile and to produce ‘bricks’ of plastic, which could be further processed into products or safely land-filled without risk to people, animals, or the environment. If melting is not an option, an all-plastic device could be disposed of by incineration using a lower temperature heat source than that required for a metal needle. For example, wood, paperboard, fuel (oil, kerosene or gasoline), or a solar oven or furnace could be used.

Plastic needles may not be as strong as metal ones. They may fail due to buckling as they are thin-walled, hollow columns. Hence the consideration of buckling is critical so as to avoid structural failure and ensure reliability for medical applications.

In this paper [10, 11], the buckling strength of plastic hypodermic needle cannulas is analysed by analytical (Euler buckling theory with correction using Johnson’s buckling formula) and finite element analysis (FEA) methods. A 22-gauge needle (OD 0.7 mm, ID 0.4 mm, length 12.7 mm) is studied. To verify the results of these analyses, cannulas with the same cross-section are fabricated using microinjection moulding, and their structural (buckling) characteristics are measured experimentally. Penetration forces through a rubber skin mimic are measured and compared to buckling loads and to reported values for human skin.

Analytic analysis

Buckling may be one cause of failure for a plastic needle; another may be tip breakage. The most critical moment during a needle’s use is just before it penetrates the skin. Here, the axial load applied to needle and the needle’s effective length are at their greatest, so any eccentricity in the loading is magnified greatly. From Euler’s buckling theory, the critical buckling load (P_{CR}) is defined as equation (1) [12].

$$P_{CR} = k \frac{EI}{L^2}, \quad (1)$$

where E is the elastic modulus of the material, I is the second moment of inertia, L is the length of the needle, and k is a constant determined by the end conditions. When a needle penetrates the skin, its end does not move because the surrounding skin prevents it from sliding. Hence, fixed-fixed ($k = 4\pi^2$) or fixed-pinned ($k = 2\pi^2$) end conditions are used in our analyses. From the needles’ dimensions and material properties, P_{CR} can be calculated. As an example, for the nylon 6-based nanocomposite used in this work (Honeywell XM-2908), which has a 4 GPa modulus, the results are summarized in table 1 for a 22-gauge needle that is 12.7 mm long. One can see the factor of two effect of the end condition on the buckling load.

Table 1. Comparison between analytic and FEA analyses for N6 nanocomposite.

	Fix-pin	Fix-fix
k (Loading condition constant)	π^2	$4\pi^2$
P_{CR} (N) (Euler)	5.725	11.193
P_{CR} (N) (Johnson corrected)	5.725	8.46
FEA results (N)	0.09	5.548
Mesh size (mm)	0.12	5.546
	0.15	5.547
Convergence of FEA	5.548	10.655
Diff (%) Euler vs. FEA	3.1	4.81

However for ‘short’ needles, the critical load calculated using equation (1) can exceed the yield load. This is because the critical load calculated using Euler’s method increases with the inverse square of the length, so as the needle is shortened, the critical buckling load increases rapidly. In addition, the moduli of the materials tend to decrease near their yield points. This increases flexibility and induces buckling at lower loads than expected. Johnson’s formula (equation (2)) relates material yield stress and Euler’s critical load to correct for these.

$$P_{CR} = A \left(S_Y - b(L)^2 \frac{A}{I} \right) \quad (2)$$

where S_Y is the compressive yield stress of the material, A is the cross-sectional area, I is the second moment of inertia, L is the length of cannula, and b is a constant evaluated by fitting a parabola between the Euler curve and the compressive yield stress [13]. The intersection point between the plot of Euler’s equation and a parabola tangent to Euler’s equation and the S_Y curve is usually set at half of S_Y . The corresponding L_{CR} at which the two curves intersect is given by equation (3) and the constant b is equation 4 for fixed-fixed end conditions. If the length of the cannula is shorter than L_{CR} , one must use equation (2) to determine the critical buckling load. Assuming that the compressive and tensile yield stresses are approximately the same, L_{CR} can be calculated for the materials used in this work using the data in table 5 for fixed-fixed end condition: polystyrene (PS) 12.0 mm, polymethylmethacrylate (PMMA) 14.7 mm, and nylon 6 nanocomposite 17.9 mm. The lengths of the needle specimens (approximately 10 mm) are smaller than critical lengths for the fixed-fixed case. For the fixed-pinned end condition, L_{CR} is $\sqrt{2}$ times less than L_{CR} for the fixed-fixed situation. Therefore, P_{CR} should be evaluated using Johnson’s buckling formula (equation (2)).

$$L_{CR} = \pi \sqrt{\frac{8EI}{AS_Y}} \quad (3)$$

$$b = \frac{1}{4E} \left(\frac{S_Y}{2\pi} \right)^2 \quad (4)$$

From these formulas, the predicted critical buckling loads for the materials are presented in table 6 below.

Finite element analysis

To obtain more accurate results and to accommodate more complex models (i.e. bevelled tip or skin-needle interface), a numerical analysis using FEA is performed using Ansys® 7.0 as follows. First, simple compression analysis is performed. From this analysis, the stiffness matrix of the cannula structure is obtained. This matrix is expanded using Lanczos’ algorithm in Ansys® to find singularities. Therefore, these procedures yield similar results to those from Euler’s method. Each of these singularities represents a mode of buckling. Ansys outputs the mode shape and its critical load.

A model of the needle is meshed using Solid 95 type elements (20 nodes per element) in different mesh sizes (0.15 mm, 0.12 mm, 0.09 mm) to verify convergence. Both fixed-pinned and fixed-fixed end conditions are analysed. For both cases, the bottom end of the needle is fixed in all directions. A 1 N force is applied as pressure on the top surface. For both conditions, all the nodes at top surface are fixed in two directions (X and Y). All the nodes at bottom surface are restricted to move in the Z direction for the fixed-fixed condition or symmetrically about the centre of the upper surface to ensure a rotational degree of freedom for the fixed-pinned case. The FEA results are summarized in table 1 for the same nanocomposite material, and table 6 for all of the materials. Figure 1 shows the deformed shape of a cannula after buckling. As seen in table 1, the FEA results agree well with the analytical buckling analyses (Euler and Johnson corrected) with less than a 10% difference.

We attempted to calculate the stress distribution at skin-needle interface using a contact analysis in Ansys®. A skin model derived from [14–17] was introduced. This model consists of four layers of different moduli and thicknesses (table 2). The stress contour plots from a simulation of poking skin with a flat tipped needle (not bevelled or sharp) (figure 2) shows that the stress is concentrated in the outer layer of the skin (stratum corneum), as this layer has the highest modulus. The resulting stress concentration factor is around 560.

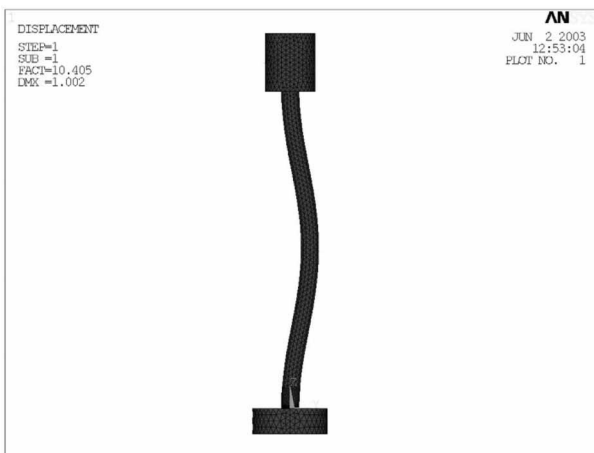


Figure 1. Buckled shape of cannula with flat ends (fixed-fixed end conditions).

Fabrication

Plastic needles (22 gauge, 0.7 mm outer diameter, 0.4 mm inner diameter, and approximately 12 mm long) were fabricated using a Sesame microinjection moulding machine (Medical Murray Inc., Buffalo Grove, IL) from various materials (polystyrene (Chevron GPPS 3600), PMMA (Atohaas Plexiglas V Grade), and nylon 6-based nanocomposite (Honeywell XM-2908)). Due to the injection capacity of the machine and the mould base size, the maximum length of the 22-gauge needle was constrained to 12.7 mm.

The mould insert was machined in a CNC milling machine. The groove that formed the needle cavity is cut using a Brothers Wirecut HS3100 WEDM (Wire Electro Discharge Machining) machine (Charmilles US, Lincolnshire, IL). WEDM is a localized heating process and leaves an oxide layer, and results in a relatively poor surface finish. Here, such a small amount of material is removed to make the mould cavity that the errors associated with the oxide layer and the deflection of the wire during cutting are significant. To correct for these errors, the groove was scraped manually with a steel needle.

Steel wire was used as the core to make a hollow needle. To align and centre this wire core, guide tubes made from small pieces of steel hypodermic needles were used. These also served as seals. These core assemblies must be attached firmly before injection moulding and be easily detached from the mould after moulding. Also, any harness structure should be very small so it can fit into mould inserts and should be heat-resistant to endure the high temperatures of

Table 2. Human skin properties.

Layer	Thickness (mm)	Young’s modulus (MPa)
Stratum corneum	0.02	12 000
Living epidermis	0.1–1.5	16
Dermis	1.5–4	12
Subcutaneous fat	1.25	20

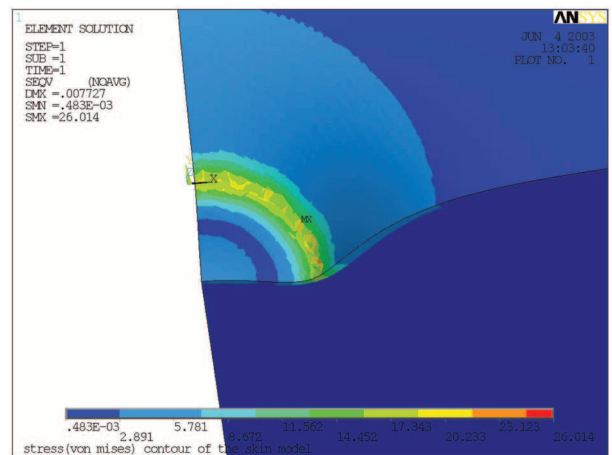


Figure 2. Stress contour of flat cannula poking skin.

the mould insert. To fulfil these requirements, a simple bottleneck design was devised. The harness assembly was made out of Teflon[®], which has good flexibility and high temperature resistance. By making the entrance bottleneck shaped, the core stayed aligned while the clamp is closing. After injection, the core with a cannula can be detached from the mould easily, because of the flexibility of Teflon[®]. By replacing one of these guide tubes with the bevelled tip of a steel needle, cannulas with the inverse shape of a steel needle tip can be made. The mould insert with its core assembly is shown in figure 3.

Before injection moulding, the plastic pellets were dried. The nylon 6-based nanocomposite material was dried more than 1 hour in an oven at 80°C and was packed in an airtight container with desiccant (silicate) pouches. PS is hydrophobic and was used without drying. PMMA was used without drying. Both the top and bottom inserts were heated above material's glass transition temperature (T_g) to facilitate mould filling. Processing conditions are presented in tables 3 and 4. The fabricated plastic needles were sharp enough to easily penetrate rubber gloves. Figure 4 shows a polystyrene needle with a bevelled tip.

Force measurement

Buckling is a phenomenon that occurs due to an unstable equilibrium. It can be observed as an abrupt change of slope in a force-displacement plot, because buckling

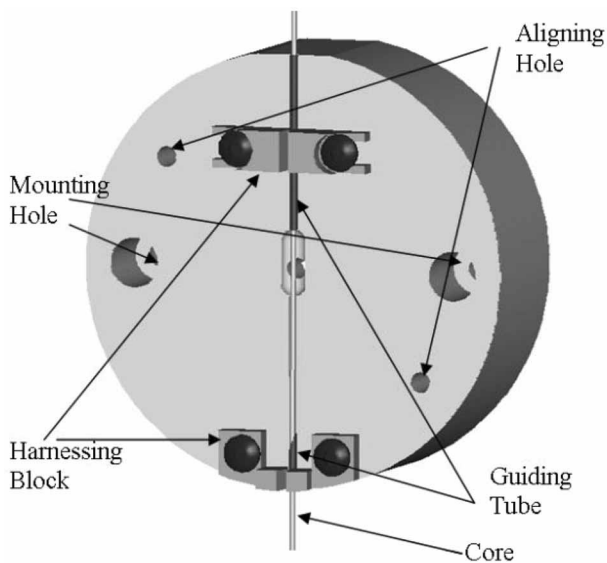


Figure 3. Mould insert assembly.

Table 3. Processing conditions.

	Polymer temperature (C)	Mould temperature (C)
N6 nanocomposite	240	93
PS	229	41
PC	277	93
PMMA	266	71

relieves the axial load by changing it into a bending moment. The buckling loads of needle cannulas (with flat tips, not bevelled) were measured by a force-displacement testing machine (Model 921A force-displacement test station, Tricor Systems Inc., Elgin, IL) equipped with a 3.6 kg force (40 N) load-cell. During testing, the needles were pressed against a rigid plate (aluminium or polycarbonate). To mimic actual conditions in which skin surrounds the needle (fixed-fixed or fixed-pinned), small pieces of the plate materials were used to form jigs to hold the needles. The plastic needles are bonded to the jigs with superglue. Also, pits were made in the plates to prevent sliding of the needle during testing. Table 6 lists the number of tests performed for each material.

For reference, the penetration forces of steel 22-gauge needles (BD model 305313, Franklin Lakes, NJ) were measured using an Instron (Canton, MA) 4466 mechanical testing machine with a 25 N load cell. Latex rubber from a rubber glove (thickness 480 μm , Ansell Edmont Industrial Inc., Coshocton, OH) was used as a skin mimic. The rubber is sandwiched firmly between two plates of Teflon-coated steel through which were cut various sized holes (6.35, 12.7, and 25.4 mm). This allowed one to determine the effect of the amount of free material; this can be related to the dent that a hypodermic needle makes before penetrating the skin. A clean needle was forced through the rubber a number of times. The penetration force was defined as the maximum force measured during each experiment.

Test results and discussion

Table 5 presents the results of the steel needle penetration of rubber tests. For the smallest sample area (6.35 mm

Table 4. Injection conditions.

Mould cool time (s)	5 s
Injection speed	1050 mm s ⁻¹
Maximum pressure	1500 Bar
Holding pressure 1	2000 Bar
Holding pressure 2	1500 Bar

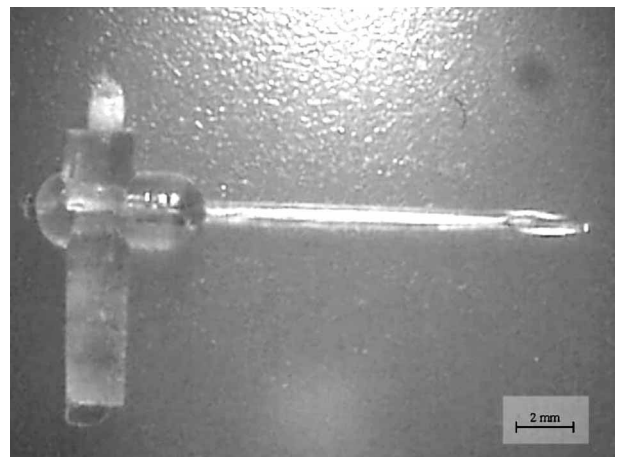


Figure 4. Polystyrene needle (needle OD = 0.7 mm).

Table 5. Steel needle penetration force.

Hole diameter of holder	Needle 1 (N)	Needle 2 (N)	Needle 3 (N)
24.5 mm	0.31	0.35 0.39	0.42 0.41
12.7 mm	0.097	0.036 0.037	0.045 0.047
6.35 mm	1.48	0.57 0.61	0.65 0.65

diameter), the maximum force required to penetrate is approximately 1.5 N. This agrees well with literature values for skin penetration of approximately 1 N [18, 19]. Hence, our rubber model is adequate for a first approximation.

Figure 5 shows a force-displacement plot of the nylon 6-based nanocomposite cannulas of different lengths. Table 6 presents the buckling test results. Note: all of the samples have fixed-fixed end conditions. The test results agree with the trend in Euler's buckling theory, that the buckling load is proportional to $1/L^2$. However, the measured buckling loads are around 75% of the loads predicted using the manufacturers' material properties and only 50% for the nylon 6-based nanocomposite. Though it is smaller than predicted, the buckling forces are at least twice as large as the penetration force required for steel 22-gauge needles in a rubber skin mimic (0.3–1.5 N), and than actual skin penetration (1 N). The penetration force depends not only on the area of the needle, but also on its sharpness (contact area of tip) [20], geometry, and lubrication. If plastic needle tip design is the same as that of a current hypodermic needle, then a plastic needle should be acceptable, as it will buckle at forces greater than 1.5 N. Therefore, we are well on the way to proving that plastic needles can indeed work for hypodermic injections.

Several explanations for the discrepancies between buckling predictions and experimental results can be offered: (1) an eccentric load due to the cannula's installation in the test fixture; (2) the cannula may have been bent during ejection from its mould; and (3) the core may have been misaligned during injection moulding. An eccentric loading induces an unwanted bending moment but it does not induce buckling at lower load. A misalignment of the core equal to the thickness of the tube wall (a physical impossibility) reduces the moment of inertia, I , by approximately 10%, hence inducing buckling at a lower load. For nylon 6-based nanocomposite, another reason may be moisture. The cannulas were stored in ambient air before testing. It is well known that moisture decreases the strength of nylons.

Conclusions

To verify the feasibility of plastic hypodermic needles, 22-gauge, 12.7 mm long cannulas are fabricated and analysed. The analytical and numerical analyses show that these cannulas can withstand between 4.5 and 10 N without buckling with both ends fixed. Actual test results yield

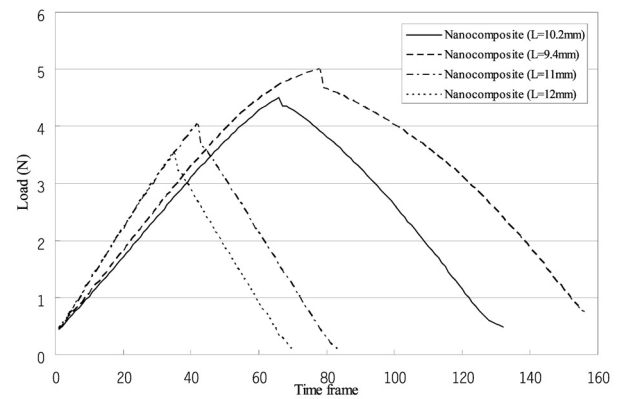


Figure 5. Force-displacement plot of nylon 6-based nanocomposite cannulas.

Table 6. Buckling results.

	Nylon 6 nanocomposite	PMMA	PS
E(GPa) (Manufacturer)	4.0	3.1	3.1
Sample length (mm)	10.2	10.8	9.5
Number of samples	4	3	3
P_{CR} (N)	Euler	17.4	12.0
	Johnson corrected	8.80	9.457
P_{CR} (measured (N))	4.47	7.09	10.02
Ratio (%) (measured to Johnson corrected)	50.8	75.0	75.1

smaller buckling loads due to eccentric loading and other reasons. However, these results are larger than the penetration force measured in penetration experiment of steel 22-gauge needles through a rubber skin mimic (0.3–1.5 N) and literature values for skin penetration (1 N). Nylon 6-based nanocomposite needles show decreases in properties due to moisture absorption. These encouraging results show that plastic needles are potential replacements for steel needles for hypodermic injections.

Acknowledgments

This research was funded in part by the Georgia Institute of Technology-Centers for Disease Control and Prevention (CDC) seed grant program. The authors thank Dr Robert T. Chen and Dr Bruce G. Weniger of the CDC for their invaluable advice.

References

- [1] Kane, A., Lloyd, J., Zaffran, M., Simonsen, L., and Kane, M., 1999, Transmission of hepatitis B, hepatitis C and human immunodeficiency viruses through unsafe injections in the developing world: model-based regional estimates. *Bulletin of the World Health Organization*, **77**, 801–807.
- [2] Simonsen, L., Kane, A., Lloyd, J., Zaffran, M., and Kane, M., 1999, Unsafe injections in the developing world and transmission of bloodborne pathogens: a review. *Bulletin of the World Health Organization*, **77**, 789–800.

- [3] Dicko, M., Oni, A. Q., Ganivet, S., Kone, S., Pierre, L. and Jacquet, B., 2000, Safety of immunization injections in Africa: not simply a problem of logistics. *Bulletin of the World Health Organization*, **78**, 163–169.
- [4] Ekwueme, D. U., Weniger, R. G. and Chen, R. T., 2002, Model-based estimates of risks of disease transmission and economic costs of seven injection devices in sub-Saharan Africa. *Bulletin of the World Health Organization*, **80**, 859–870.
- [5] Miller, M. A. and Pisani, E. 1999, The cost of unsafe injections. *Bulletin of the World Health Organization*, **77**, 808–811.
- [6] Dziekan, G., Chisholm, D., Johns, B., Rovira, J., and Hutin, Y., 2003, The cost-effectiveness of policies for the safe and appropriate use of injection in healthcare settings. *Bulletin of the World Health Organization*, **81**, 277–285.
- [7] Nelson, C. M., Sutanto, A. and Suradana, I. G. P., 1999, Use of Solo-shot autodestruct syringes compared with disposable syringes, in a national immunization campaign in Indonesia. *Bulletin of the World Health Organization*, **77**, 29–33.
- [8] World Health Organization, 1999, Safety of injections, WHO-UNICEF-UNFPA joint statement on the use of auto-disable syringes in immunizations services. WHO/V&B/99.25.
- [9] Mujeeb, S. A., Adil, M. M., Altaf, A., Hutin, Y. and Luby, S., 2003, Recycling of injection equipment in Pakistan. *Infection Control and Hospital Epidemiology*, **24**, 145–146.
- [10] Kim, H., 2004, Fabrication and analysis of plastic hypodermic needles by micro injection molding, M.Sc. thesis, Atlanta: Georgia Institute of Technology.
- [11] Kim, H. and Colton, J. S., 2004, Fabrication and analysis of plastic hypodermic needles. *Proceedings of Annual Technical Conference, Society of Plastics Engineers*, 16–20 May 2004, Brookfield, CT, Chicago, pp. 3727–3731.
- [12] Gere, J. M. and Timoshenko, S. P., 1999, *Mechanics of Materials* (Cheltenham, UK: Stanley Thrones).
- [13] Shigley, J. E., and Mischke, C. R., 1989, *Mechanical Engineering Design* (New York, USA: McGraw-Hill).
- [14] Oomens, C. W. J., Bressers, F. J. T., Bosboom, E. M. H. and Bouten, C. V. C., 2001, Deformation analysis of a supported buttock contact. *Proceedings of the 2001 Bioengineering Conference*, American Society of Mechanical Engineers, BED Vol. 50. Snowbird, Utah, 27 June–1 July. 853–854.
- [15] Heinrich, T. and Lunderstaedt, R. A., 2000, Quantification of mechanical properties of human skin in vivo. *Proceedings SPIE*, **4472**, 11–20.
- [16] Douven, L. F. A., Meijer, R., and Oomens, C. W. J., 2000, Characterization of mechanical behavior of human skin in vivo. *Proceedings SPIE*, **3914**, 618–629.
- [17] Hendriks, F. M., Brokken, D., Van Eemeren, J., Oomens, C. W. J., Baaijens, F. P. T. and Horsten, J. B. A. M., 2003, A numerical-experimental method to characterize the non-linear mechanical behaviour of human skin. *Skin Research and Technology*, **9**, 274–283.
- [18] Frick, T. B., Marucci, D. D., Cartmill, J. A., Martin, C. J. and Walsh, W. R., 2001, Resistance forces acting on suture needles. *Journal of Biomechanics*, **34**, 1335–1340.
- [19] Kataoka, H., Washio, T., Chinzei, K., Mizuhara, K., Simone, C., and Okamura, A. M., 2002, Measurement of the tip and friction force acting on a needle during penetration. *Proceedings of the International Conference on Medical Image Computing and Computer Assisted Intervention*, Lecture notes in computer science, **2488**, 216–223.
- [20] Davis, S. P., 2003, Hollow microneedles for molecular transport across skin, Ph.D. Thesis, Atlanta: Georgia Institute of Technology.